

# Atomic structure, electrical properties, and infrared range optical properties of diamondlike carbon films containing foreign atoms prepared by pulsed laser deposition

Q. Wei and J. Sankar

*NSF Center for Advanced Materials and Smart Structures, Department of Mechanical Engineering, North Carolina A&T State University, Greensboro, North Carolina 27411*

A.K. Sharma, S. Oktyabrsky, and J. Narayan

*Department of Materials Science and Engineering, North Carolina State University, Raleigh, North Carolina 27695-7916*

R.J. Narayan

*Department of Medicine, Wake Forest University, Winston Salem, North Carolina 27106*

(Received 25 June 1999; accepted 20 December 1999)

We investigated the atomic structure, electrical, and infrared range optical properties of diamondlike carbon (DLC) films containing alloy atoms (Cu, Ti, or Si) prepared by pulsed laser deposition. Radial distribution function (RDF) analysis of these films showed that they are largely  $sp^3$  bonded. Both pure DLC and DLC + Cu films form a Schottky barrier with the measuring probe, whereas DLC + Ti films behave like a linear resistor. Pure DLC films and those containing Cu exhibit  $p$ -type conduction, and those containing Ti and Si have  $n$ -type conduction. Photon-induced conduction is observed for pure DLC, and the mechanism is discussed in terms of low-density gap states of highly tetrahedral DLC. Our results are consistent with relative absence of gap states in pure DLC, in accordance with theoretical prediction by Drabold *et al.*<sup>37</sup> Temperature dependence of conductivity of DLC + Cu shows a behavior  $\sigma \propto \exp(-B/T^{1/2})$ , instead of the  $T^{-1/4}$  law (Mott–Davis law). Contributions from band-to-band transitions, free carriers, and phonons to the emissivity spectrum are clearly identified in pure DLC films. The amorphous state introduces a large contribution from localized states. Incorporation of a small amount of Si in the DLC does not change the general feature of emissivity spectrum but enhances the contribution from the localized states. Cu and Ti both enhance the free carrier and the localized state contributions and make the films a black body.

## I. INTRODUCTION

The range of different forms of carbon, such as diamond, graphite, fullerenes, nanotubes, and DLC, etc., has made carbon one of the most interesting elements in nature.<sup>1</sup> The great variety of structures and the unique properties of carbon stem from its unique chemistry, i.e., the capability of forming various types of hybridization that can be used to form different bonding states.<sup>2</sup> The beneficial properties of DLC are due to the  $sp^3$  bonding constituents that make DLC mechanically hard, infrared (IR) transparent, and chemically inert.<sup>3</sup> High-quality DLC films can rival diamond films in terms of mechanical performance such as wear resistance, very low coefficient of friction, high hardness, and elastic modulus.<sup>4</sup> Furthermore, unlike polycrystalline diamond films prepared by chemical vapor deposition (CVD) and other techniques, DLC films are usually very smooth. Owing to their unique properties, DLC films have found appli-

cations as hard protective coatings for magnetic disk drives, as antireflective coatings for infrared windows, as field emission source, and so on.<sup>5–7</sup> A number of investigations have confirmed that ultraviolet (UV) pulsed laser ablation of a high-purity polycrystalline graphite target is able to produce high-quality DLC films with a Tauc gap of  $\sim 1.8$ – $2.0$  eV and an  $sp^3/sp^2$  ratio of  $\sim 80\%$ .<sup>8–10</sup> The special feature of pulsed laser ablation is that it is a nonequilibrium process and the species produced in the laser plasma possess very high kinetic energy. For instance, the average kinetic energy of atomic species produced by equilibrium processes such as electron beam evaporation is around  $\sim kT$  ( $k$  is the Boltzmann constant, and  $T$  is the absolute temperature), whereas that produced by pulsed laser ablation might be as high as  $100$ – $1000kT$ .<sup>11</sup> Therefore, pulsed laser deposition (PLD) is one of the techniques to make high-quality DLC thin films without the requirement of hydrogen incorporation

and in some aspects is superior to filtered cathodic vacuum arc (FCVA)<sup>12</sup> and mass-selected ion beam (MSIB) deposition<sup>13</sup> techniques.

The main stumbling block for the application of DLC films as protective coatings is the accumulation of a high amount of compressive stress into the overconstrained amorphous network. Recently, we tried to address this challenging problem by incorporating small fractions of foreign atoms in the amorphous structure of DLC.<sup>14,15</sup> The adhesion and wear resistance of DLC films were improved substantially upon doping. This was achieved without significantly affecting the diamondlike properties of the films.

Since one of the major applications of DLC films is IR window coatings, it is crucial to understand the IR range optical properties of DLC films that have dopants. It should be noted that even though a number of studies have been reported on the IR measurements of DLC films, the films were in most cases hydrogenated.<sup>16</sup> The study of electrical properties of the doped DLC films and the effect of light on those properties will also be very useful to correlate optical properties and to explore the possibility of fabricating photodiodes from these films.

In the present work, several aspects of pure DLC films and those containing various types of dopants prepared by PLD were studied. We investigated the atomic structure of these films by means of radial distribution function (RDF) analysis, the IR range optical properties through emissivity measurements, and temperature-dependent conduction behavior. We used Rutherford backscattering spectroscopy (RBS) and x-ray photoelectron spectroscopy (XPS) to acquire chemical composition of the DLC films. Visible Raman spectroscopy was used to study the bonding characteristics and the effect of dopant incorporation. A spectral emissometer that can collect radiance, reflectance, and transmittance simultaneously was used to analyze the IR range optical properties. The  $I$ - $V$  characteristics of the DLC films were measured and preliminary observations of photon irradiation effect on conduction were performed. Conduction mechanisms were studied via temperature-dependent resistivity measurements. The results were discussed to present a unified understanding of the phenomena.

## II. EXPERIMENTAL PROCEDURES

### A. Materials and pulsed laser deposition

A novel target configuration described elsewhere<sup>14</sup> was adopted to incorporate various dopants into DLC films during PLD. The  $p$ -type silicon(100) wafers were used as substrates. The doping of DLC films was accomplished using ingenious modification of pulsed laser deposition. A strip of doping element is placed on the rotating target, where the relative amounts of target and dopant constituents are determined by the scanning ra-

dius of the laser beam, energy density, and optical reflectivity of the target and the dopant strip. Copper, titanium, and silicon were chosen as dopants because Cu is not a carbide former, whereas Ti is a strong carbide former with metallic bonding with carbon, and Si is all  $sp^3$  bonded, having covalent bonding and electronic structure similar to  $sp^3$  bonded carbon and is also a carbide former. The Si wafers were cleaned in acetone and methanol ultrasonic baths followed by HF dip to remove the native oxide layer before loading into the laser deposition chamber. The laser beam was pulsed excimer laser ( $\lambda = 248$  nm,  $t_s = 25$  ns) at a repetition rate of 10 Hz, with an energy density close to  $3.0$  J/cm<sup>2</sup>. All the depositions were performed at room temperature for 40 min in a high vacuum of about  $1 \times 10^{-7}$  torr.

### B. Film characterization

Transmission electron microscopy (TEM) studies were conducted using TOPCON002B microscope at 200 kV with a point-to-point resolution of  $1.8$  Å at the first Scherzer defocus. RDF analysis was based on digitizing intensities of the electron diffraction patterns and calculating the reduced density functions. Both RBS and XPS were used for estimating chemical composition of the doped films. Visible Raman (514.7 nm) spectroscopy and XPS were employed to study the chemical bonding states of different films.

Room-temperature emissivity measurements were performed to study the IR range optical behavior of the films using a Benchtop spectral emissometer that can acquire radiance, reflectance, and transmittance simultaneously. The detailed instrumentation of IR measurements was described by Ravindra *et al.*<sup>17</sup> A method based upon Seebeck effect was used to determine the conduction type of the DLC alloys. The  $I$ - $V$  characteristics and the influence of light on the conduction of several films were analyzed. The low-temperature resistivity as a function of cryogenic temperature was recorded using equipment that is used for the characterization of superconductor materials (for example, critical temperature measurements). The setup is equipped with a cryopump that is able to cool the sample to near liquid-He temperature.

## III. RESULTS AND DISCUSSION

First, we will present the results pertaining to the chemical composition of the films, such as RBS and XPS. Also included in this part are the Raman spectroscopy results on both doped and pure DLC films. Microstructural information obtained by TEM and RDF on several samples will be presented in the next part. The third part will consist of electrical measurements such as conductivity,  $I$ - $V$  characteristics, and results of photon irradiation effect on conduction and resistivity as a function of temperature. The final part will be focused on the IR range optical studies and the effect of dopants.

## A. Chemical composition and bonding of the DLC films

Simulations of the RBS results showed that the atomic fraction of Cu in a DLC + Cu film is 1.2 at.% and that of Ti in a DLC + Ti film is 2.75 at.%. Compositional analysis by XPS for these two samples gives 1.44 at.% Cu and 2.66 at.% Ti, respectively, consistent with the RBS results. The thickness of all the films was in the range 400–600 nm. Composition of the films can be controlled through changing either the scanning radius of the laser beam on the surface of the target or the size of the dopant piece on the target. The composition results for different depositions are given in Table I. Due to the presence of particulates in the DLC + Si films, we did not attempt to obtain the content of Si in these films.

Figure 1 presents the visible Raman spectra for several samples with different dopants and for the undoped DLC film, showing a broad hump centered in the range 1510–1560  $\text{cm}^{-1}$  and extending to 1300  $\text{cm}^{-1}$ . These are typical of Raman spectra for an amorphous carbon, with little or no long range order. Namely, there are no well-developed graphitic nanocrystallites above about 2 nm in size, except for the DLC + Ti film, in which the D-component contribution is relatively large. The G-peak position of the doped films shifts to the smaller wave numbers. According to Praver *et al.*,<sup>18</sup> the position of the G-peak is a function of  $sp^2$  content for pure, hydrogen-free DLC. For very low  $sp^2$  content, the G-peak position does not change significantly. Since the majority of samples in the present work contain foreign atoms, the method developed by Praver *et al.*<sup>18</sup> is not applicable.

We have shown<sup>14</sup> in the XPS of Cu in the DLC film that contains Cu two peaks due to Cu 2p<sub>1/2</sub> and Cu 2p<sub>3/2</sub> with binding energies of 952.6 and 933.7 eV, respectively, with no evidence of carbide formation or Cu–C bonding. For XPS of DLC + Ti, however, apart from the peaks corresponding to Ti 2p orbital electrons at binding energies of 460 and 454 eV, two shoulders close to them are also observed at 460.9 and 454.7 eV, respectively. These shifts in the binding energies of Ti 2p<sub>3/2</sub> (454 eV) and Ti 2p<sub>1/2</sub> (460 eV) toward the high-binding energy side provide evidence of Ti and carbon bonding. The outer shells of a Ti atom are  $3d^24s^2$ , and it might be envisaged that this shell configuration could contribute to the change of short-range electronic structure of DLC and thus give rise to the change of Raman spectrum.

TABLE I. Concentration of dopants in the DLC films (at.%).

Sample no.	Dopants						
	Copper				Titanium		
	Cu-O	Cu-1	Cu-2	Cu-3	Ti-1	Ti-2	Ti-3
Concentration	1.2	1.4	1.5	2.5	2.7	4.0	7.7

## B. Microstructure and RDF analysis of the DLC films

Figure 2 is the TEM image of DLC with 1.2 at.% Cu, and the corresponding electron diffraction pattern shows typical features of amorphous state.

RDF analysis enables us to get information of the first and second coordination spheres such as the distances of the first and second nearest neighbors and the coordination numbers, etc.<sup>19</sup> In the case of DLC, since it possesses both fourfold and threefold coordination, the first

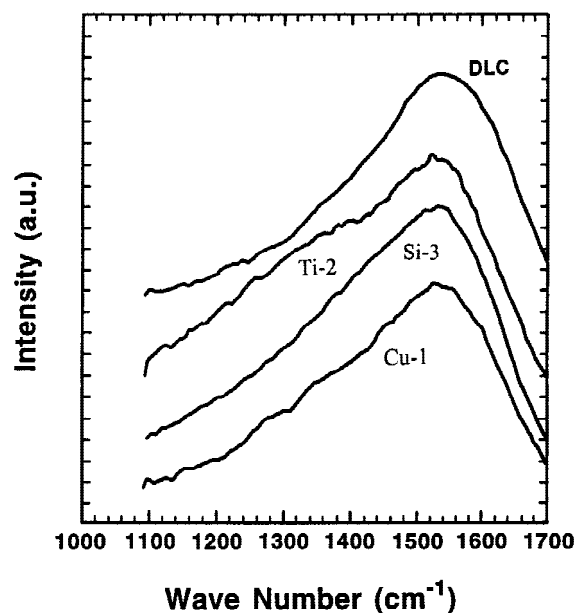


FIG. 1. Visible Raman spectra of several DLC films.

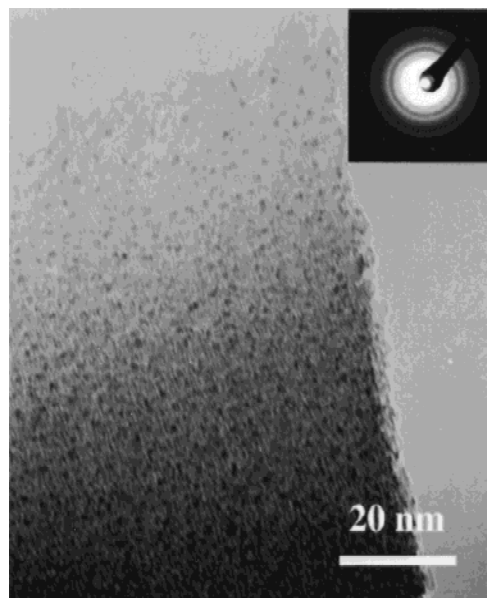


FIG. 2. TEM micrograph and electron diffraction pattern (inset) of DLC + 1.2 at.% Cu film.

and second coordination spheres in the RDF should have coordination numbers between those of graphite (3, 6) and those of diamond (4, 12).

Figure 3 shows the RDF calculated from the electron diffraction data of pure DLC. The first and second nearest-neighbor distances as obtained from the RDF analysis are 1.51 and 2.52 Å, respectively. The ratio of the second shell coordination number to the first shell coordination number is approximately 2.75. In a comparison of these data with those of diamond and graphite, it is clear that the pure DLC should possess a significant percentage of  $sp^3$ -bonded carbon atoms. Figure 4 shows the RDF for the DLC film with 1.2 at.% Cu. For this sample, the first and second nearest-neighbor distances are 1.50 and 2.54 Å, respectively, while the ratio of the second shell coordination number to the first shell coordination number is approximately 2.84. The structural data imply that the presence of copper atoms does not change the short-range environment significantly. In Table II, the results of RDF analysis, such as first nearest-neighbor distance, second nearest-neighbor distance, and the ratio of first- to second-shell coordination numbers, are given. Also given in Table II are data for diamond, graphite, and amorphous carbon made by other techniques. By comparison of the first and second nearest-neighbor distances and coordination numbers to those of diamond and graphite, it is clear that the DLC films consist mainly of  $sp^3$ -bonded carbon.

So far, the number of diffraction studies on highly tetrahedral carbon is quite limited.<sup>24,25</sup> One example is the work by Gaskell *et al.*,<sup>24</sup> who used neutron diffraction on DLC films made by the filtered direct current (dc) vacuum arc (FDVA) technique. Their DLC films had the

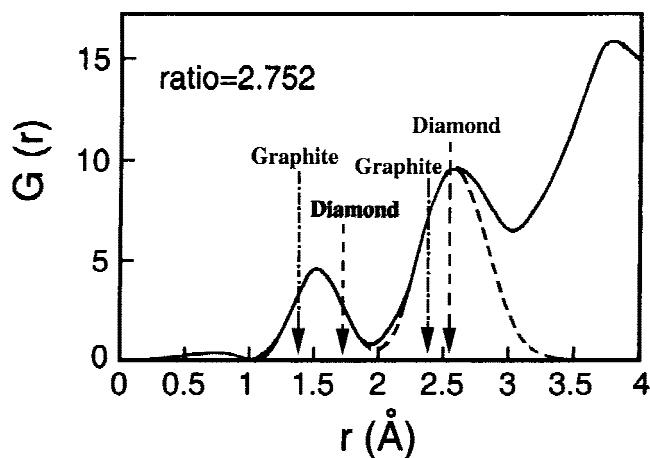


FIG. 3. Radial distribution function (RDF) of pure DLC. The dashed line is for the calculation of coordination numbers. For comparison, the first and second nearest-neighbor distances of diamond are 1.544 and 2.512 Å, and the ratio of the first to the second shell coordination number is 3, while the first and second nearest-neighbor distances of graphite are 1.42 and 2.45 Å, respectively, and the ratio of the first to the second shell coordination number is 2.

first nearest-neighbor distance of 1.52 Å and the ratio of first- to second-shell coordination numbers of 2.80. Most of the other RDF analyses have been based upon amorphous carbon films that are predominantly trigonally bonded. For example, Li and Lannin<sup>21</sup> studied the RDF of thick amorphous carbon films prepared by radio frequency (rf) sputtering in a high-vacuum environment. The macroscopic density of the a-C films was estimated from weighing selected samples to be only 2.0 g/cm<sup>3</sup>, and the film thickness was about 4 μm. Optical absorption and reflectance measurements yielded a Tauc gap of 0.57 eV. All these features merely imply that the a-C films were not of high content of fourfold coordination. They analyzed the RDF obtained by neutron diffraction and obtained 1.46 and 2.49 Å as the first and second nearest-neighbor distances, respectively. RDF analyses by Boiko *et al.*<sup>26</sup> were based on electron diffraction of amorphous carbon films prepared by the method of vacuum evaporation. The integration to compute the RDF was carried out up to a maximum scattering vector of 8.8 Å<sup>-1</sup>. In their calculation, they took the density of amorphous carbon as  $\rho_0 = 2.1$  g/cm<sup>3</sup> and calculated the coordination numbers for the respective spheres to be  $3.3 \pm 0.2$  and  $8.8 \pm 0.2$ . These results suggest that the amorphous carbon films are predominantly composed of trigonally bonded carbon.

In their theoretical studies of DLC, Wang *et al.*<sup>27</sup> generated an amorphous carbon network by quenching high-density high-temperature liquid carbon using tight-

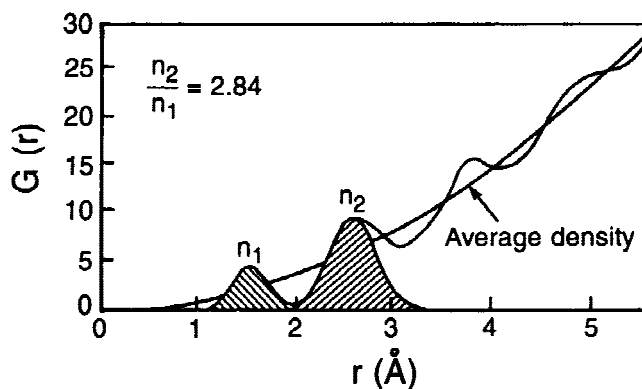


FIG. 4. RDF of DLC + Cu film. The DLC film contains 1.2 at.% Cu. The shaded area is for the calculation of coordination numbers.

Table II. Results of RDF analysis and comparison with other C forms.

Carbon phases	$r_1$ , Å	$r_2$ , Å	$n_2/n_1$	Refs.
Graphite	1.42	2.45	2	20
a-C (sputtered)	1.46	2.49	2.1	21
Glassy (carbon)	1.425	2.45	2.1	20
a-C (evaporated)	1.43	2.53	2.6	23
Diamond	1.544	2.512	3	22
Pure DLC	1.51	2.52	2.75	This work
DLC + 1.2%Cu	1.50	2.54	2.8	This work

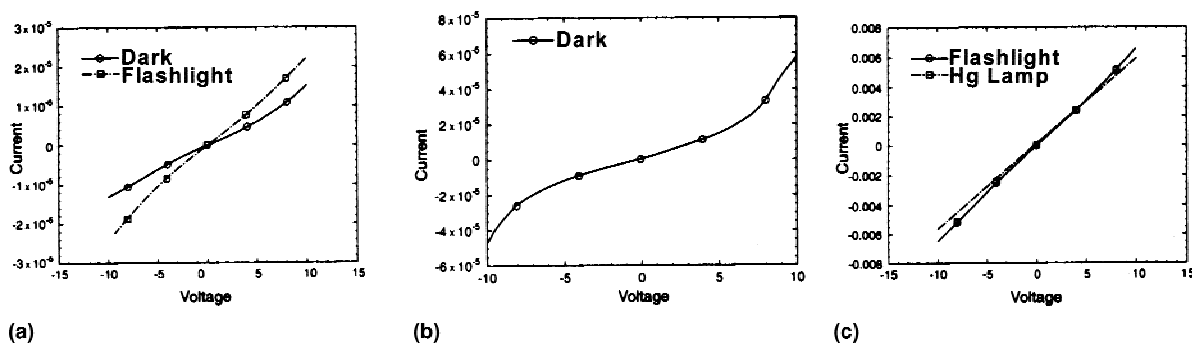


FIG. 5. Current–voltage characteristics of (a) pure DLC film, (b) DLC + 2.5 at.% Cu, and (c) DLC + 2.7 at.% Ti films. Also shown in these curves is the light effect on conduction of the pure DLC film.

binding molecular dynamics simulations. They found that the network so created contains a large fraction of  $sp^3$  sites (74%). The results of structural analysis are quite close to our experimental observations. For example, their RDF analyses of the model structure yield the first peak at 1.52 Å. The structural analysis of the present work is also consistent with that by Frauenheim *et al.*<sup>28</sup> and supported by electron energy loss spectroscopy (EELS),<sup>29</sup> as well as by nanoindentation measurements<sup>15</sup> that gave a hardness close to 50 GPa and reduced Young’s modulus greater than 200 GPa.

### C. Electrical properties of the DLC films

Four-probe measurements showed that the resistance of the DLC films does not change linearly with dopant concentration,<sup>30</sup> in agreement with that in Ref. 31. Amorphous semiconductors usually have all states localized, and their conduction exhibits hopping, especially variable-range hopping mechanism. The hopping probability can be expressed as<sup>32</sup>

$$w_{ij} = w_0 \exp\left(-\frac{2R}{\lambda} - \frac{W}{kT}\right), \quad (1)$$

where  $w_0$  is a constant,  $R$  is the distance the electron crosses by tunneling in one hopping event;  $\lambda$  is a measure of the extent of the state (localization length),  $W$  is the thermal activation energy,  $k$  is Boltzmann constant, and  $T$  is absolute temperature. Equation (1) indicates that the hopping probability and thus the conductivity of the material will be increased with decreased  $R$ . When the concentration of foreign atoms that can contribute to localized states is increased, the distance that the electron will cross over one tunneling event would be smaller, leading to a reduced resistivity. When the concentration of these atoms is increased to such a level that continuous channels might be formed for the transport of electrons, the films could essentially behave like metallic materials.

It is found that pure DLC films exhibit  $p$ -type conduction, which is in agreement with other investigations.<sup>33</sup> DLC films containing copper also exhibit  $p$ -type conduc-

tion. Generally, Cu has been reported to act as an acceptor in most semiconductors.<sup>34</sup> For example, it has three acceptor levels in crystalline silicon. Therefore, it is not surprising that DLC films containing Cu also shows  $p$ -type conduction.

Figure 5 shows the  $I$ – $V$  characteristics of (a) pure DLC, (b) DLC containing 2.5 at.% Cu, and (c) DLC containing 2.7 at.% Ti. It can be seen that all the films except the one containing Ti form a Schottky contact with the measuring probe. The DLC + Ti sample simply exhibits metallic conduction as a resistor, with its  $I$ – $V$  curve following Ohm’s law. This can in part be understood in connection with the XPS observation that Ti–C bonding is present in the film. As is known, Ti–C bonding is essentially metallic and its presence might greatly enhance the conduction of the film by increasing the density of states near the Fermi level,  $E_F$ . Also seen in Fig. 5 is the effect of light on conduction (photoconduction) of the pure DLC film. Further investigations are continuing regarding the photoconduction of DLC films containing foreign atoms.

For other tetrahedral amorphous semiconductors such as Si and Ge, doping is very difficult if they are not hydrogenated due to the presence of a large population of dangling bonds.<sup>35</sup> However, highly tetrahedral amorphous carbon formed by energetic C ions is shown to have a relatively low density of defect gap states.<sup>36,37</sup> This allows ta-C to be doped and show photoconductivity, even without hydrogenation. Electron spin resonance (ESR) measurements have shown that the spin density of DLC decreases with increasing  $sp^3$  bonding. Amaratunga *et al.*<sup>36</sup> ascribed the low defect density of ta-C that contains 10–40%  $sp^2$  sites to the ability of  $sp^2$  sites to pair up and form  $\pi$  bonds. The states of these  $\pi$  bonds lie outside the gap. As pointed out by Drabold,<sup>37</sup> the defect-free gap and high  $sp^3$  count are the most interesting features of ta-C. Their modeling suggests a significant proclivity for the  $sp^2$  atoms to pair up and thus be swept out of the 2-eV gap and to sweep out other defect states with them. More specifically, the  $sp^2$  “defects” form pairs in which one of the two hybridized states is pushed lower in energy and

one is pushed higher in energy. Since only the lower energy state is occupied, the total energy is significantly lowered. Further, there is some tendency for the  $\pi$ -bonded pairs to form short chains. Therefore, single  $sp^2$  atoms, or dangling bonds, do not occur in substantial numbers as they do in a-Si. It also appears that defect states associated with geometric anomalies are also pushed out of the  $sp^2$  gap into the band edges of the diamond or  $sp^3$  gap, that is, what would have also hybridized with the  $sp^2$  states and are thus pushed out of the gap. From Fig. 5, the pure DLC film exhibits some light-induced conduction.

As pointed out by Sullivan and Friedmann,<sup>38</sup> electronic transport in amorphous carbon largely bonded by  $sp^3$  hybridization has been the subject of considerable debate. There are generally three mechanisms of conduction in amorphous semiconductors, which may be found in appropriate ranges of temperature:<sup>35</sup> (i) transport is by carriers excited beyond the mobility edges into extended states at  $E_c$  or  $E_v$ ; (ii) transport is by carriers excited into localized states at the band edges and hopping at energy close to  $E_A$  or  $E_B$  ( $E_A$  and  $E_B$  define the localization induced tail-end of the band edges;  $E_A$  is below  $E_c$ , and  $E_B$  is above  $E_v$ ); (iii) if the density of states (DOS) at  $E_F$  is finite, then there will be a contribution from carriers with energies near  $E_F$  which can hop between localized states by the process analogous to impurity conduction in heavily doped crystalline semiconductors. At temperatures such that  $kT$  is less than the bandwidth, hopping will not necessarily be between nearest neighbors and variable-range hopping of the form

$$\sigma = \sigma'_2 \exp(-B/T^{1/4}) \quad , \quad (2)$$

with B a constant depending upon the DOS at  $E_F$  is to be expected, at a temperature sufficiently low for  $N(E_F)$  to be considered constant over an energy range  $\sim kT$ .

Figure 6 presents the curve showing the relation between  $\ln(\ln \sigma)$  and  $\ln(1000/T)$  of the DLC film that contains 1.2 at.% Cu. It is clear that two regimes are present in Fig. 6. The first regime corresponds to higher temperature conduction close to room temperature, and the second, to low-temperature conduction. The data for the latter regime are well fit by the relation

$$\sigma \propto \exp\left(-\frac{B}{T^{1/2}}\right) \quad , \quad (3)$$

where B is a constant. This temperature dependence of conductivity in disordered systems has also been observed in other materials.<sup>39,40</sup> This behavior can be understood on the basis of the theory developed by Efros and Shklovskii,<sup>41</sup> who derived the  $\sim T^{-1/2}$  dependence by considering the long-range Coulomb interactions between the localized states. According to their model, the DOS should not be a constant near the Fermi level, as is

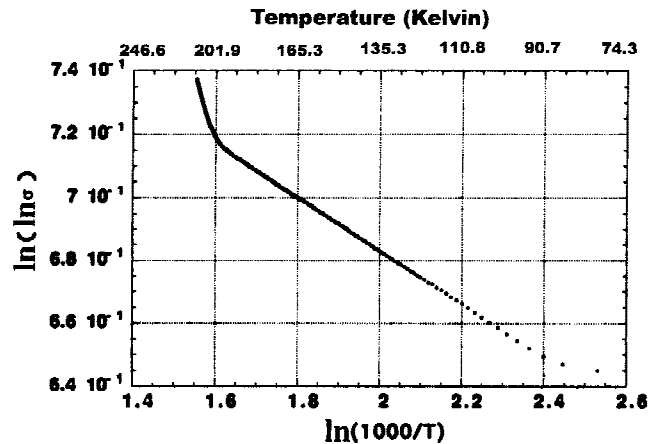


FIG. 6. Relation between  $\ln(\ln \sigma)$  versus  $\ln(1000/T)$  of DLC film that contains 1.2 at.% Cu.

the essential assumption in the derivation of the Mott-Davis law ( $T^{-1/4}$  behavior). Their more realistic model states that the DOS at  $|E - E_F| < \Delta$  ( $\Delta$  is the gap) decreases with  $|E - E_F|$  and should vanish at the Fermi level. The value of  $\Delta$  determines the critical temperature  $T_C$  below which the  $\sim T^{-1/2}$  behavior should prevail. Hamilton *et al.*<sup>42</sup> reported similar behavior in amorphous carbon. In most cases,  $T_C$  is very low and  $\sim T^{-1/2}$  dependence can be observed only below liquid-nitrogen temperature. In the present work,  $\sim T^{-1/2}$  dependence exists close to room temperature. This may be explained as a manifestation of the Coulomb gap according to Efros and Shklovskii.<sup>41</sup>

While several investigations reported  $\sim 1/T^{1/4}$  behavior of electrical conduction, the carbon films were mostly made by near-equilibrium techniques such as electron beam evaporation, arc evaporation, or plasma-assisted chemical vapor deposition.<sup>43,44</sup> Such carbon films could be expected to mainly consist of three-fold carbon. It is therefore not certain whether they can be used to represent DLC films prepared via nonequilibrium techniques such as pulsed laser deposition since the structures, either atomically or electronically, are very different.

We therefore envisaged that the copper atoms in the DLC films act as Coulomb interaction centers, which results in the  $\sim T^{-1/2}$  behavior.

#### D. IR range optical properties of the DLC films

Emissivity is defined as the ratio of the radiance of a given object to that of a black body at the same temperature and for the same spectral and directional conditions.<sup>45</sup> It is a function of wavelength and temperature. For normal incidence, the emissivity  $\epsilon$  of a plane parallel specimen could be written as

$$\epsilon = \frac{(1 - R)(1 - T_r)}{1 - RT_r} \quad , \quad (4)$$

where  $R$  is the true reflectivity and  $T_r$  is the true transmissivity. They are related to the fundamental optical parameters such as the refractive index  $n$  and the extinction coefficient  $k$ . For a perfect opaque body, for example when  $\alpha t$  ( $\alpha$  is the absorption coefficient, and  $t$ , the thickness of the specimen) is large and  $T_r \approx 0$ , we have the Kirchhoff's law as

$$\epsilon = 1 - R = \frac{4n}{(n+1)^2 + k^2} \quad (5)$$

If the apparent reflectivity and transmissivity that are actually measured experimentally are denoted by  $R^*$  and  $T_r^*$ , the following relation holds:

$$\epsilon + R^* + T_r^* = 1 \quad (6)$$

There are generally three contributions to the emittance of a semiconductor, i.e., band-to-band transitions, free carriers, and phonons (lattice vibrations). In the case of a defect-free crystalline semiconductor such as intrinsic silicon, these three contributions are distinct from one another at low temperatures where the concentration of free carriers is still low. The emissivity increases abruptly when the photon energy exceeds the band gap.

Figure 7(a) shows emittance of pure DLC measured near room temperature. The emittance spectrum exhibits three regimes. The first regime corresponds to large wave numbers (higher photon energies) that shows high emittance. Though DLC films prepared by 248-nm excimer laser with high laser fluence ( $\sim 10 \text{ J/cm}^2$ ) have been reported to have a band gap of  $\sim 1.5 \text{ eV}$ , Dikshit *et al.*<sup>31</sup> reported a value close to  $1.0 \text{ eV}$  on DLC films prepared under the same laser fluence as the present work. We may therefore attribute the first regime to band-to-band transitions. Apart from this, however, in the case of amorphous semiconductors, there are a large number of localized states, especially close to the band edges. We might expect that these localized states would also contribute to emittance. This is indeed what happens to DLC where no sharp transitions are observed in the emittance spectrum. Instead, gradual changes are present. The second regime is from free carriers, while the third regime of wavelength close to  $10 \mu\text{m}$  is due to phonon contribution. The emissivity due to free carriers is governed by the impurity concentration of the semiconductor, the thickness of the specimen, and also by the temperature at which the specimen is kept. For a crystalline intrinsic semiconductor like silicon, free carrier contribution increases with temperature. When the specimen is doped, this contribution can also be enhanced significantly.

Incorporation of small amount of Si into DLC films does not change the general features of the emissivity and transmittance spectra, as shown in Fig. 7(b). However, it is found that it contributes slightly to the localized state

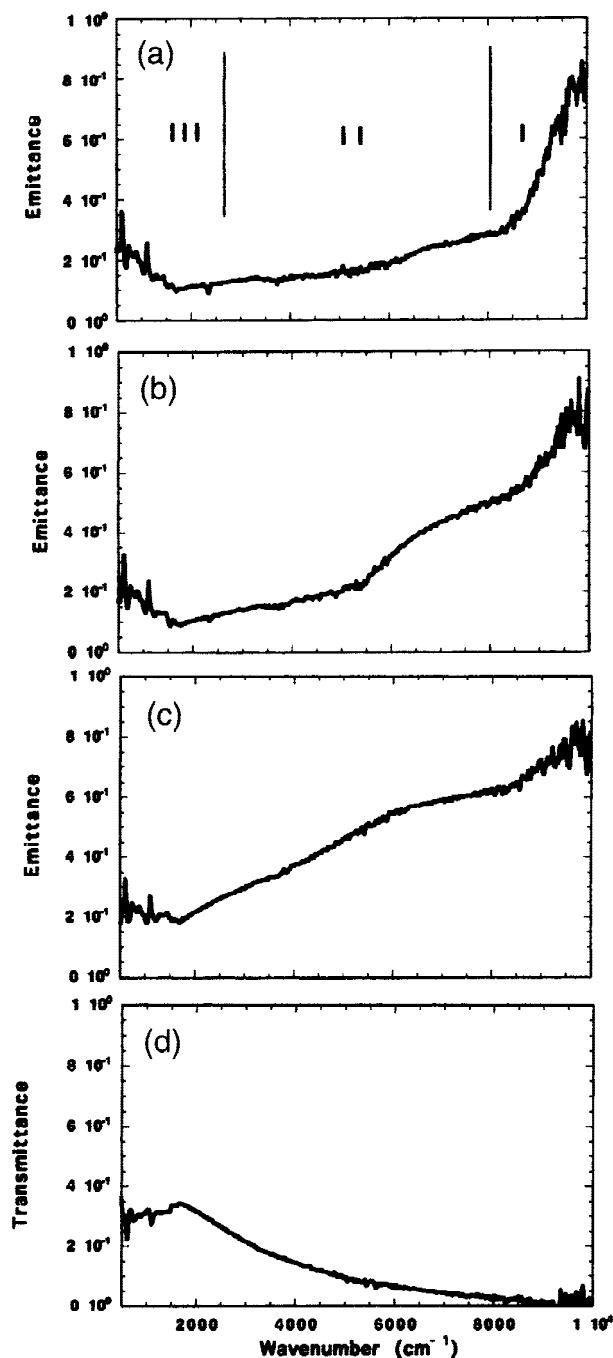


FIG. 7. IR range emissivity spectra of (a) pure DLC, (b) DLC + Si, and (c) DLC + Cu (1.4 at.% Cu) films, showing the emittance (%) as a function of wave number. Three regimes are indicated in the spectrum for pure DLC. In (d) is the transmittance spectrum of DLC + Ti (2.7 at.% Ti) that shows that the film is opaque.

part starting from wave number  $5500 \text{ cm}^{-1}$ . It also contributes a little to the free carrier part. This effect is increased with Si content. It is understood that Si has tetrahedral bonding and the lone pair electrons may contribute to the free carrier concentration. This understanding is in accordance with electrical measurements, which

show that the presence of Si increases the electrical conductivity of DLC.<sup>30</sup> It is also consistent with the fact that intrinsic DLC is a *p*-type semiconductor whereas Si-incorporated DLC shows *n*-type conduction.

The emittance of DLC containing small amount of Cu [Fig. 7(c)] shows significant increase in the whole range of measurement, while the transmittance in the IR range is considerably decreased so that the film is almost opaque. Most probably the increase of the contribution from free carriers has far exceeded the contribution from increased localized states, though the contribution from the localized states could still be discerned from the emittance spectrum. This can be identified from the gradual increase of emissivity with wave number. It was also found that the effect of doping increases with increasing Cu content. This could be understood in connection with the electrical conduction behavior of DLC films containing Cu where the conductivity increases with Cu content.

Ti-incorporated DLC films behave almost as a black body [Fig. 7(d)], where the transmittance just goes to zero, and here Kirchhoff's law can be applied. The emissivity is almost independent of wave number. Free carriers suppress all contributions from band-to-band transitions, from localized states and from phonons. In other words, the emitted radiation from other contributions might have been absorbed before it reaches the specimen surface. It is found that DLC + Ti exhibits *n*-type conduction. The outer-shell structure of Ti is  $3d^2 4s^2$ , and the outer-shell electrons can contribute to the free carrier concentration and remarkably increase the electron concentration in the film and make the film opaque. This is consistent with *I*-*V* characteristics of these samples that shows DLC + Ti acts essentially as a resistor, with the *I*-*V* curve following Ohm's law. Also the evidence for Ti-C bonding as established by XPS gave the same binding energies as bulk titanium carbide. Since TiC has metallic bonding, the IR optical behavior of DLC + Ti films is consistent with our observations.

#### IV. SUMMARY AND CONCLUDING REMARKS

The atomic structure, IR range optical properties, and several aspects of the electrical properties of diamondlike carbon films containing foreign atoms prepared by pulsed laser deposition were studied. RDF analyses of the electron diffraction show that the films were predominantly bonded by fourfold coordination, with the first and second nearest distances being quite close to those of crystalline diamond. The *I*-*V* characteristics of pure DLC and DLC + Cu indicate that both form a Schottky barrier with the measuring probe, whereas the Ti-doped DLC behaves just like a linear resistor. Pure DLC exhibits *p*-type conduction. Ti- and Si-doped DLC films

have *n*-type conduction, while Cu-doped DLC films show *p*-type conduction. A light effect on conduction is observed for pure DLC. The mechanism of light-induced conduction is discussed in terms of the gap states of pure DLC. Our results may be considered to verify a clean gap of pure DLC, in accordance with the theoretical prediction by Drabold *et al.*<sup>37</sup> Measurements on the temperature dependence of conductivity of DLC + Cu show the following behavior  $\sigma \propto \exp(-B/T^{1/2})$  instead of the  $T^{-1/4}$  law (Mott-Davis law). Infrared optical measurements showed three contributions to the emissivity spectrum of pure DLC. They include band-to-band transitions, free carriers, and phonons (lattice vibrations). The amorphous state introduces a large contribution due to the presence of the localized states. Incorporation of a small amount of Si in the DLC does not change the general feature of emissivity spectrum but enhances the contribution from the localized states. Ti enhances the free carrier concentration as well as the localized state contributions to the extent that the films behave as a black body.

#### ACKNOWLEDGMENTS

We thank Dr. Ravindra for fruitful discussions and help with the IR measurements. This research is sponsored by the National Science Foundation under Contract No. CMS 9414434.

#### REFERENCES

1. P. Ball, *Nature* **391**, January 8, 1998.
2. P.W. Atkins, *Physical Chemistry*, 5th ed. (W.H. Freeman, San Francisco, CA, 1994).
3. J. Robertson, *Prog. Solid Stat Chem.* **21**, 199 (1991).
4. A.A. Voevodin and M.S. Donley, *Surf. Coat. Technol.* **82**, 199 (1996).
5. W.I. Milne, *J. Non-Cryst. Solids* **198-200**, 605 (1996).
6. K. Enke, *Mater. Sci. Forum* **52-53**, 559 (1990).
7. *Covalently Bonded Disordered Thin-Film Materials*, edited by M.P. Siegal, W.I. Milne, and J.I. Jaskie (Mater. Res. Soc. Symp. Proc. **498**, Warrendale, PA, 1998).
8. J. Krishnaswamy, A. Rengan, J. Narayan, K. Vedom, and C.J. McHorgue, *Appl. Phys. Lett.* **54**, 2455 (1989).
9. J. Sato, S. Furuno, S. Ifuchi, and M. Hanabusa, *Jpn. J. Appl. Phys.* **26**, 1487 (1987).
10. D.L. Pappas, K.L. Saenger, J. Bruley, W. Krakow, and J.J. Cuomo, *J. Appl. Phys.* **71**, 5672 (1992).
11. E.A. Rohlfing, *J. Chem. Phys.* **89**, 6103 (1988).
12. M. Chhowalla, Y. Yin, G.A.J. Amaratunga, D.R. McKenzie, and Th. Frauenheim, *Diamond Relat. Mater.* **6**, 207 (1997).
13. J. Kulik, Y. Lifshitz, G.D. Lempert, J.W. Rabalais, and D. Marton, *J. Appl. Phys.* **76**, 5063 (1994).
14. Q. Wei, R.J. Narayan, J. Narayan, S. Sankar, and A.K. Sharma, *Mater. Sci. Eng. B* **53**, 262 (1998).
15. Q. Wei, R.J. Narayan, A.K. Sharma, J. Sankar, and J. Narayan, *J. Vac. Sci. Technol.* **17**, 3406 (1999).
16. K. Ebihara, T. Ikegami, T. Matsumoto, H. Nishimoto, S. Maeda, and K. Harada, *J. Appl. Phys.* **66**, 4996 (1989).

17. N.M. Ravindra, S. Abedrabbo, W. Chen, F.M. Tong, A.K. Nanda, and A.C. Speranza, *IEEE Trans. Semicond. Manufact.* **11**, 30 (1998).
18. S. Prawer, K.W. Nugent, Y. Lifshitz, G.D. Lempert, E. Grossman, J. Kulik, I. Avigal, and R. Kalish, *Diamond Relat. Mater.* **5**, 433 (1996).
19. D.J.H. Cockayne and D.R. McKenzie, *Acta Crystallogr. A* **44**, 870 (1988).
20. D.F.R. Mildner and J.M. Carpenter, *J. Non-Cryst. Solids* **47**, 391 (1982).
21. F. Li and J.S. Lannin, *Phys. Rev. Lett.* **65**, 1905 (1991).
22. J.E. Field, *Properties of Diamond* (Academic Press, San Diego, CA, 1979).
23. D.C. Green, D.R. McKenzie, and P.B. Lukins, *Mater. Sci. Forum*, **52–53**, 103 (1990).
24. P.A. Gaskell, A. Saeed, P. Chieux, and D.R. McKenzie, *Phys. Rev. Lett.* **67**, 1286 (1991).
25. D.R. McKenzie, D. Muller, and B.A. Pailthorpe, *Phys. Rev. Lett.* **67**, 773 (1991).
26. B.T. Boiko, L.S. Palatnik, and A.S. Derevyanchenko, *Sov. Phys. Dokl.* **13**(3), 237 (1968).
27. C.Z. Wang and K.M. Ho, *Phys. Rev. Lett.* **71**, 1184 (1993).
28. Th. Frauenheim, P. Blaudech, U. Stephan, and G. Jungnickel, *Phys. Rev. B* **48**, 4823 (1993).
29. A.F. Myers, M.Q. Ding, S.M. Camphausen, W.B. Choi, J.J. Cuomo, and J.J. Hren, in *Covalently Bonded Disordered Thin-Film Materials*, edited by M.P. Siegal, W.I. Milne, and J.I. Jaskie (*Mater. Res. Soc. Symp. Proc.* **498**, Warrendale, PA, 1998), p. 83.
30. Q. Wei (unpublished work).
31. S.J. Dikshit, P. Lele, S.B. Ogale, and S.T. Kshirsagar, *J. Mater. Res.* **11**, 2236 (1996).
32. O. Madelung, *Introduction to Solid-State Theory* (Springer, Berlin, 1996).
33. P. Fallon, V.S. Veerasamy, C.A. Davis, J. Robertson, G.A.J. Amaratunga, W.I. Milne, and J. Koskinen, *Phys. Rev. B* **48**, 4877 (1993).
34. A.G. Milnes, *Deep Impurities in Semiconductors* (John Wiley & Sons, New York, 1973).
35. N.F. Mott and E.A. Davis, *Electronic Processes in Non-crystalline Materials*, 2nd ed. (Clarendon Press, Oxford, United Kingdom, 1979).
36. G.A.J. Amaratunga, J. Robertson, V.S. Veerasamy, W.I. Milne, and D.R. McKenzie, *Diamond Relat. Mater.* **4**, 637 (1995).
37. D.A. Drabold, P.A. Fedders, and M.P. Grumbach, *Phys. Rev. B* **54**, 5480 (1996).
38. J.P. Sullivan and T.A. Friedmann, in *Specialist Meeting on Amorphous Carbon* (Cambridge University, World Scientific, Singapore, 1997).
39. J. Stankiewicz, S. von Molnar, and W. Giriat, *Phys. Rev. B* **33**, 3573 (1986).
40. W.N. Shafarman, T.G. Castner, J.S. Brooks, K.P. Martin, and M.J. Naughton, *Phys. Rev. Lett.* **56**, 980 (1986).
41. A.L. Efros and B.I. Shklovskii, *J. Phys. C: Solid State Phys.* **8**, L49 (1975).
42. E.M. Hamilton, J.A. Cross, and C.J. Adkins, in *Proceedings of the International Conference on Amorphous and Liquid Semiconductors*, edited by J. Stuke and W. Brenig (Taylor & Francis, London; Halsted Press, New York 1974), p. 1225.
43. A. Bozhko, A. Ivanov, M. Berrettoni, S. Chudinov, S. Stizza, V. Dorfman, and B. Pypkin, *Diamond Relat. Mater.* **4**, 488 (1995).
44. R. Grigorovici, A. Devenyi, A. Gheorghia, and A. Belu, *J. Non-Cryst. Solids* **8–10**, 793 (1972).
45. T. Sato, *Jpn. J. Appl. Phys.* **6**, 339 (1967).